

Cover Page



Universiteit Leiden



The handle <http://hdl.handle.net/1887/43472> holds various files of this Leiden University dissertation

**Author:** Waaijer, Mariëtte

**Title:** The skin as a mirror of the aging process

**Issue Date:** 2016-10-12



# Chapter 6

---

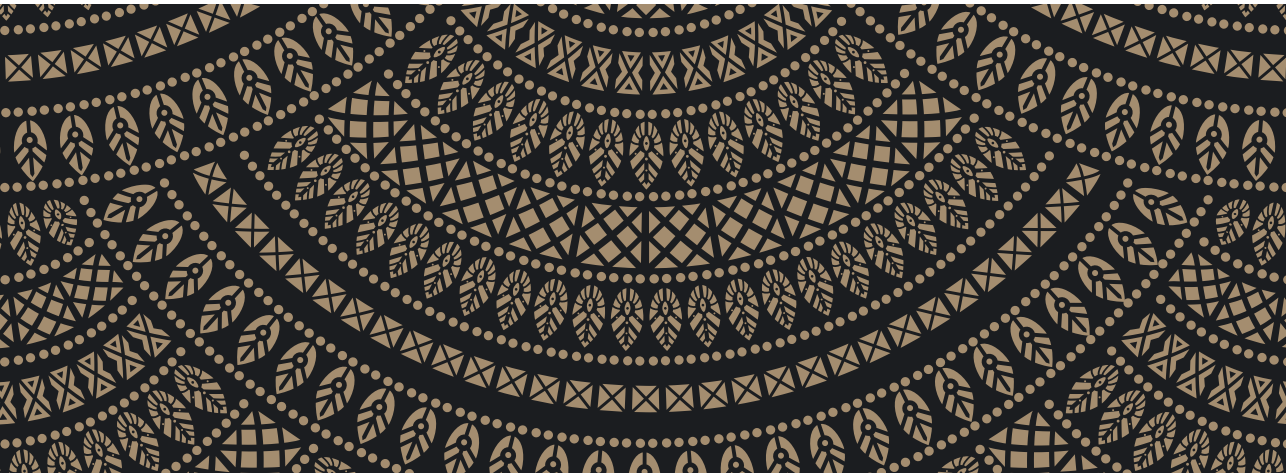
## Chapter 6

### **P16INK4a positive cells in human skin are indicative of local elastic fibre morphology, facial wrinkling and perceived age**

M.E.C. Waaijer\*, D.A. Gunn\*, P.D. Adams, J.S. Pawlikowski, C.E.M. Griffiths,  
D. van Heemst, P.E. Slagboom, R.G.J. Westendorp, A.B. Maier

\* Both authors contributed equally

*Journal of Gerontology: Biological Sciences* 2016 Aug;71(8):1022-8



## Abstract

Senescent cells are more prevalent in aged human skin compared to young, but evidence that senescent cells are linked to other biomarkers of ageing is scarce. We counted cells positive for the tumour suppressor and senescence associated protein p16INK4a in sun-protected upper inner arm skin biopsies from 178 participants (45-81 years of age) of the Leiden Longevity Study. Local elastic fibre morphology, facial wrinkles and perceived facial age were compared to tertiles of p16INK4a counts, whilst adjusting for chronological age and other potential confounders.

The numbers of epidermal and dermal p16INK4a positive cells were significantly associated with age-associated elastic fibre morphologic characteristics, such as longer and a greater number of elastic fibres. The p16INK4a positive epidermal cells (identified as primarily melanocytes) were also significantly associated with more facial wrinkles and a higher perceived age. Participants in the lowest tertile of epidermal p16INK4a counts looked 3 years younger than those in the highest tertile, independently of chronological age and elastic fibre morphology.

In conclusion, p16INK4a positive cell numbers in sun-protected human arm skin are indicative of both local elastic fibre morphology and the extent of ageing visible in the face.

## **Introduction**

Cellular senescence can be described as the inability of mammalian cells to undergo replication due to stable cell cycle arrest. Cells senesce in response to a variety of stresses such as DNA damage, oxidative stress and telomere shortening<sup>1</sup>. The relevance of cellular senescence to ageing has been shown in several animal models<sup>2-4</sup> and in humans<sup>5-7</sup> where the prevalence of senescent cells was higher in old compared to young tissues. Furthermore, links have been observed between senescent cells and biological age – an individual's physiological condition irrespective of their chronological age, for example due to beneficial familial characteristics or disease. We demonstrated that the offspring of nonagenarian siblings, who have a propensity for longevity, have less p16INK4a positive cells in the epidermis and dermis of upper-inner arm skin than aged-matched controls<sup>8</sup>. In addition, other studies have shown that higher p16INK4a expression levels in transplanted kidneys are predictive of worse transplant function<sup>9</sup>, and p16INK4a positivity was associated with hypertensive histological changes in the kidney<sup>10</sup> and type 2 diabetic nephropathy<sup>11</sup>. A higher prevalence of senescent cells has also been linked to atherosclerosis<sup>12</sup> and lung emphysema<sup>13</sup>. Finally, removal of p16INK4a positive cells delayed the onset and progression of age-related disease in progeroid mice<sup>14</sup> supporting the notion that the presence of senescent cells can be detrimental to tissues.

The tissue with the most visible signs of deterioration with age is the skin which is accompanied by marked changes to its morphology. For example, the epidermis flattens and the number and size of elastic fibres increase with age<sup>15</sup>. How old an individual looks for their age (perceived facial age) is influenced not only by changes to skin morphology but also by subcutaneous changes that affect face shape such as the appearance of the nasolabial fold and facial sag<sup>16-19</sup>. About 50% of the variation in perceived age can be attributable to skin wrinkling<sup>16</sup> whereas the rest of the variation is likely predominately due to changes in face shape. Although skin wrinkling is strongly influenced by sun exposure<sup>20-23</sup>, perceived age is also linked to ageing and disease. Higher perceived age associates with lower survival<sup>24</sup>, higher glucose levels<sup>25</sup>, higher cortisol levels<sup>26</sup>, higher blood pressure in women<sup>27</sup> and increased carotid atherosclerosis<sup>28</sup>; and human familial longevity in men was associated with a lower perceived age<sup>27</sup>.

Here, we studied whether the number of cells positive for the senescence associated protein p16INK4a in sun-protected upper inner arm skin, associated with local skin morphology and the extent of ageing visible in the face, i.e. facial wrinkles and perceived age. We hypothesised that higher numbers of p16INK4a positive cells in human skin would be associated with skin morphology typical in older individuals, more facial wrinkles and a higher perceived age independently of potential confounders such as age and smoking.

## Methods

The study design of the Leiden Longevity Study (LLS) and all methodologies have been described previously<sup>8;15;29;30</sup>; we briefly describe the design below. Data from 178 LLS randomly selected participants were used in this study.

### *Study design*

The LLS consists of men and women over 89 and 91 years of age respectively with at least one sibling who passes the same age criterion, the offspring of either long-lived sibling and the partners of the offspring (i.e. married to/civil partnership with the offspring)<sup>30</sup>. The offspring and their partners were the subjects in this study. The study protocol was approved by the Medical Ethics Committee of the Leiden University Medical Centre (following the declaration of Helsinki) and participants gave informed written consent.

### *Skin biopsies – p16INK4a staining and counting*

Skin biopsies (4 mm) were taken from the sun-protected site of the upper-inner arm and fixed in formalin (Sigma) overnight (18–24 h). Biopsies were washed, dehydrated, embedded in paraffin wax and cut into 4 µm sections. As described previously<sup>8</sup>, p16INK4a staining was carried out using the E6H4 antibody<sup>31</sup> as per the manufacturer's instructions (CINtec Histology Kit, MTM Laboratories). Counting of p16INK4 positive cells was carried out along

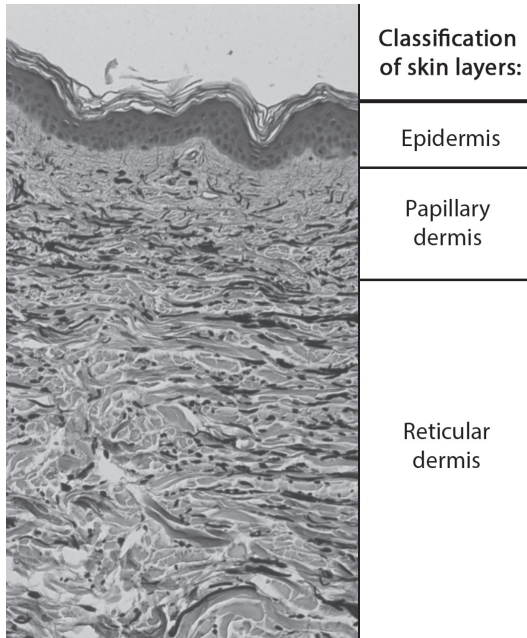


**Figure 1.** Example of a skin biopsy section with the classification of layers used in the study.

In this skin biopsy section stained with Orcein dye the epidermis and dermis were demarcated by defining the epidermal-dermal junction. The dermis was divided into depth layers of 100 micrometre, where layer 1 represented the papillary dermis and layers 2 to 5 the reticular dermis.

the full length of the epidermis and adjusted for the length of the epidermal-dermal junction. As all cells were located immediately above the basal membrane, no correction for epidermal depth was required. To identify the epidermal p16INK4a positive cell-type, dual staining for p16INK4a and S100 (X0311 Dako; a marker of melanocyte and Langerhans cells) was carried out on the same skin sections and positive cells along the basal membrane were counted. In addition, we stained skin sections for p16INK4a and MelA (clone A103, M7196 Dako, a more specific marker for melanocytes in the skin than S100) and examined adjacent sections for co-localisation of staining. Both methods have been detailed previously<sup>32</sup> and were carried out on 3 participants. For dermal cell counts, cell identification and counting was carried out in the papillary and upper to mid reticular areas using a 40 X objective. Counts were restricted to nucleated linear or oval cells morphologically determined as fibroblasts, and corrected for the measurement area.

#### *Skin biopsies – morphology*

The measurement of skin morphology characteristics has been described previously<sup>15</sup>. Two sections of each biopsy were stained with Orcein dye and the resulting skin sections imaged and assessed for epidermal and elastic fibre morphology. Epidermal measurements included the thickness of the epidermis (image area covered by epidermis divided by the length of the epidermal–dermal junction) and the curvature in the epidermis (the ratio of a straight line between the horizontal margins of the epidermis over the length of the stratum corneum–epidermis boundary). Within the dermis, the area covered by the elastic fibres and their number (both corrected for the size of image area they were measured in) as well as the area (micrometre squared), length (micrometre), thickness (micrometre) and the curl of an elastic fibre (the ratio between its length and the calliper dimension) were measured. The dermis was divided into depth layers of 100 micrometre, layer 1 represented the papillary dermis and layers 2 to 5 the reticular dermis (Figure 1). Due to the variability in skin biopsy thickness, the number of available subjects for skin morphology varied: N=177 for epidermis and papillary dermis, N=175 for reticular dermis.

#### *Measurement of facial features*

Wrinkle grading of the facial images was carried out as previously reported<sup>16</sup> utilising grading from two skin ageing experts; the mean value was used for further analyses. The methodology used for generating perceived facial age has been reported in detail elsewhere<sup>16;29</sup>. In brief, an en-face and a 45 degree photograph of the face were acquired for all participants (without the presence of any facial products), the images cropped around the neck and hair line before being presented, in a randomised order, to naive age assessors via a computer screen where they chose a 5-year age range dependent on how old they thought the participants looked. All participating assessors were unaware of presentation designs, subject ages and age ranges.

The mean perceived ages were generated from an average of 60 independent assessments of age (range: 59-61 assessments). Inter-rater reliability of the perceived age assessment was excellent (Cronbach's alpha 0.99).

#### *Demographic characteristics*

For each subject, demographic and lifestyle characteristics were obtained. Information on medical history (available for N=161-169 dependent on condition) was obtained from the participants' treating physicians, including history of myocardial infarction, stroke, hypertension, diabetes mellitus, malignancy, rheumatoid arthritis and chronic obstructive pulmonary disease. Information on skin-type (skin goes red, pink or tans upon sun exposure), sun exposure (how often one sunbathes and is outside) and sun bed use (number of occasions one uses a sun bed per year), body mass index (BMI, weight in kg/length in m<sup>2</sup>) and smoking status (smokers include both former and current smokers, data available for N=169) was collected via questionnaires.

#### *Statistics*

All statistical analyses were performed with IBM SPSS Statistics 20 software. As the p16INK4a counts were not normally distributed, the data was divided into three equal-sized data subsets (low: N=59, middle: N=60, high: N=59) for the analyses. These tertiles of p16INK4a positivity were calculated for the epidermis and dermis separately. The tertiles of p16INK4a positive epidermal cells were distributed as following: lowest  $\leq 0.30$  (median = 0.00), middle 0.30–1.30 (median = 0.55), highest  $\geq 1.30$  (median = 3.09) cells per mm length of the epidermal–dermal junction. For the tertiles of p16INK4a positive dermal fibroblasts: lowest  $\leq 0.72$  (median = 0.00), middle 0.72–2.05 (median = 1.29), highest  $\geq 2.05$  (median 3.20) cells per 1 mm<sup>2</sup> dermis. For simplicity and as a reflection of overall morphology, composite scores were generated for morphology characteristics of the epidermis and elastic fibres in both the papillary and reticular dermis separately. For this, Z-scores of all skin morphology characteristics were calculated and added; the Z-scores of epidermal thickness and dermal curl of elastic fibres had inverse associations with age so were multiplied by -1 (see <sup>15</sup>). Hence, a higher elastin morphology composite score reflected a combination of elastic fibre characteristics associated with a greater chronological age.

To estimate skin morphology composite score means for each p16INK4a tertile and to calculate the P-value for trend, linear mixed models were used. In model 1, adjustments were made for age, sex and long-lived family member status. For model 2, model 1 was expanded with further adjustments for skin tanning type, sun bed use, sun exposure (although the skin was from a sun-protected site, these adjustments ensured sun exposure influences on the data was minimal), smoking, and BMI; we also adjusted for the number of cardiovascular and

metabolic diseases (including cerebrovascular accident, myocardial infarction, hypertension and diabetes mellitus) as we previously found links between such parameters and number of p16INK4a cells in skin <sup>8</sup>. The wrinkle grading and perceived age adjustment models 1 and 2 were as described above. Model 3, however, included an additional adjustment for the elastic fibre morphology composite scores of both the papillary and reticular dermis. Also for perceived age only, model 4 consisted of model 3 plus adjustment for the wrinkle grading.

**Table 1.** Characteristics of the study participants

	N=178
Age <sup>a</sup> , years	63.4 (6.6)
Male <sup>b</sup>	88 (49.4)
Long-lived family member <sup>b</sup>	89 (50.0)
Skin tanning type <sup>b</sup>	
Red	75 (42.1)
Pink	62 (34.8)
Tans	41 (23.0)
Sun bed use <sup>b</sup>	
Never	127 (71.3)
1-5 times per year	29 (16.3)
≥ 6 times per year	22 (12.4)
Sun exposure <sup>b</sup>	
Rarely outside	23 (12.9)
Often outside	113 (63.5)
Mostly outside	42 (23.6)
Former and/or current smokers <sup>b</sup>	105 (62.1)
Co-morbidities <sup>b</sup>	
Myocardial infarction	3 (1.8)
Cerebrovascular accident	7 (4.3)
Hypertension	43 (26.4)
Diabetes mellitus	11 (6.8)
Malignancy	6 (3.7)
Chronic obstructive pulmonary disease	6 (3.7)
Rheumatoid arthritis	0 (0.0)
Body mass index <sup>a</sup> , kg/m <sup>2</sup>	26.5 (3.8)

Data are depicted as either <sup>a</sup>: mean (standard deviation) or <sup>b</sup>: number (%).

## Results

Table 1 shows the characteristics of 178 study participants. The mean age of participants was 63 years with equal numbers of men and women, and half were members of a long-lived family (i.e. the offspring), while the other half consisted of their partners.

Since the association with the number of p16INK4a positive cells and chronological age has been described previously, we examined whether this could be confirmed in our cohort. In an univariate analysis, tertiles of epidermal p16INK4a positivity were positively associated with chronological age (P for trend=0.023), but tertiles of dermal p16INK4a positivity were not associated (P for trend =0.964).

We next investigated whether the number of p16INK4a positive cells associated with local skin morphology, facial wrinkles and perceived age. Epidermal p16INK4a positivity was not associated with epidermal morphology, but was positively associated with the dermal elastic fibre morphology in the papillary dermis even after adjustment for potential confounders (Table 2 and Figure 2: P for trend <0.001, model 2). A trend between epidermal p16INK4a positivity and dermal elastic fibre morphology in the reticular dermis was seen in model 1 (P for trend=0.064), and after adjustment for further confounders a positive association was observed (P for trend=0.016, model 2). Likewise, dermal p16INK4a positivity was not associated with epidermal morphology but was associated with the elastic fibre morphology in both the papillary and reticular dermis (Table 2 and Figure 2: P for trend =0.041 and P for trend =0.010 respectively, model 2). Analyses using each individual skin morphological characteristic rather than a composite score demonstrated similar associations (Supplementary tables 1 and 2).

Next, we assessed the association of p16INK4a positivity tertiles with wrinkle grading and perceived age. Higher tertiles of epidermal p16INK4a positivity were significantly associated with a higher mean wrinkle grade, even after adjustment for potential confounders including the papillary and reticular elastic fibre composite scores (Table 3 and Figure 2: P for trend =0.033, model 3). Furthermore, higher tertiles of epidermal p16INK4a positivity were associated with a higher perceived age (P for trend =0.005, model 3). The trend remained after adjustment for the wrinkle grading (one of the components of perceived age) (Table 3: P for trend =0.076, model 4). Dermal p16INK4a positivity was not significantly associated with the wrinkle grading or perceived age (Table 3 and Figure 2), although there was a tendency for it to associate with perceived age after adjusting for the wrinkle grading (Table 3: P for trend = 0.064, model 4).

**Table 2.** Skin morphology composite scores dependent on tertiles of P16INK4a positivity.

	Tertiles of epidermal p16INK4a positivity			P for trend	Tertiles of dermal p16INK4a positivity			P for trend
	Low ≤0.30	Middle 0.30-1.30	High ≥1.30		Low ≤0.72	Middle 0.72-2.05	High ≥2.05	
Composite score – Epidermis								
Model 1	-0.27 (0.21)	0.13 (0.20)	-0.10 (0.21)	0.803	-0.09 (0.20)	0.03 (0.20)	0.06 (0.20)	0.596
Model 2	-0.24 (0.25)	-0.10 (0.27)	-0.22 (0.27)	0.922	-0.42 (0.26)	-0.04 (0.26)	-0.11 (0.27)	0.337
Composite score - Papillary dermis, layer 1								
Model 1	-1.14 (0.55)	-0.81 (0.54)	1.94 (0.55)	<0.001	-1.05 (0.57)	0.74 (0.56)	0.30 (0.56)	0.103
Model 2	-1.45 (0.65)	-0.96 (0.70)	2.59 (0.59)	<0.001	-1.24 (0.73)	0.65 (0.72)	0.58 (0.77)	0.041
Composite score - Reticular dermis, layers 2 to 5								
Model 1	-0.50 (0.57)	-0.57 (0.57)	1.05 (0.57)	0.064	-1.36 (0.57)	0.87 (0.56)	0.48 (0.56)	0.027
Model 2	-0.82 (0.70)	-0.70 (0.77)	1.32 (0.76)	0.016	-1.67 (0.73)	0.84 (0.72)	0.66 (0.76)	0.010

All values are given as estimated mean with standard error (SE). Estimated means were calculated by using a linear mixed model: model 1: adjustment for age, sex and long-lived family member status; model 2: as model 1 plus skin tanning type, sunbed use, sun exposure, smoking, number of cardiovascular and metabolic diseases and body mass index. See supplementary material for the individual skin morphology characteristics dependent on p16INK4a positivity. Epidermal p16INK4a positivity: number of cells staining positive for p16INK4a per mm length of the epidermal–dermal junction, dermal p16INK4a positivity: number of cells staining positive for p16INK4a per 1 mm<sup>2</sup> dermis

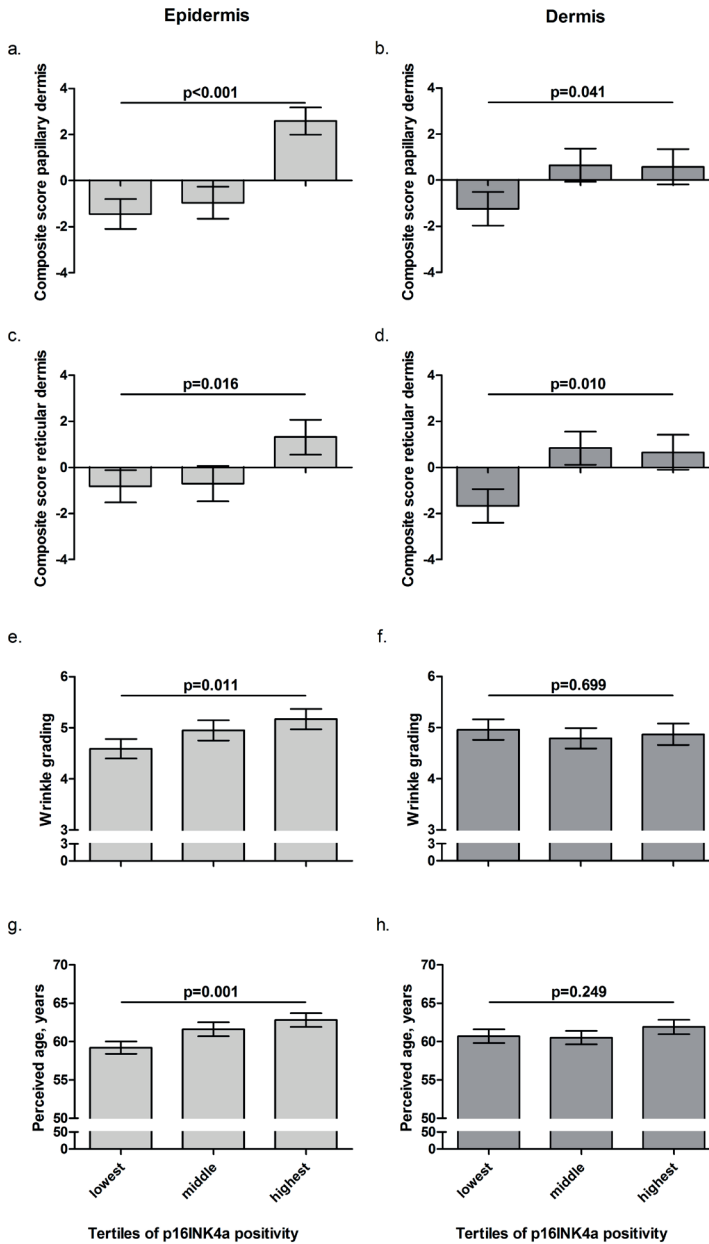


**Figure 2.** Elastic fibre composite scores, wrinkle grading and perceived age dependent on tertiles of p16INK4a positivity.

All values are given as estimated mean  $\pm$  standard error. Estimated means were calculated with a linear mixed model. Adjustment was made for chronological age, sex, long-lived family member status, skin tanning type, sunbed use, sun exposure, smoking, number of cardiovascular diseases and body mass index.

**Table 3.** Wrinkle grading and perceived age dependent on tertiles of p16INK4a positivity.

	Tertiles of epidermal p16INK4a positivity			P for trend	Tertiles of dermal p16INK4a positivity			P for trend
	Low ≤0.30	Middle 0.30-1.30	High ≥1.30		Low ≤0.72	Middle 0.72-2.05	High ≥2.05	
<b>Wrinkle grading</b>								
Model 1	4.47 (0.15)	4.77 (0.15)	5.04 (0.15)	0.007	4.88 (0.15)	4.76 (0.15)	4.66 (0.14)	0.301
Model 2	4.59 (0.19)	4.95 (0.20)	5.17 (0.20)	0.011	4.96 (0.20)	4.79 (0.20)	4.87 (0.21)	0.699
Model 3	4.63 (0.19)	4.90 (0.20)	5.15 (0.21)	0.033	4.99 (0.20)	4.78 (0.20)	4.84 (0.20)	0.565
<b>Perceived age (in years)</b>								
Model 1	58.9 (0.68)	60.3 (0.67)	62.2 (0.68)	0.001	60.3 (0.70)	60.4 (0.69)	60.7 (0.69)	0.656
Model 2	59.2 (0.83)	61.6 (0.90)	62.8 (0.89)	0.001	60.7 (0.90)	60.5 (0.89)	61.9 (0.94)	0.249
Model 3	59.4 (0.83)	61.5 (0.90)	62.4 (0.93)	0.005	60.9 (0.90)	60.3 (0.87)	61.7 (0.93)	0.400
Model 4	59.7 (0.62)	60.9 (0.66)	61.1 (0.69)	0.076	60.0 (0.65)	60.1 (0.63)	61.4 (0.65)	0.064

All values are given as estimated mean with standard error (SE). Estimated means were calculated by using a linear mixed model: model 1: adjustment for age, sex and long-lived family member status; model 2: as model 1 plus skin tanning type, sunbed use, sun exposure, smoking, number of cardiovascular diseases and body mass index; model 3: as model 2 plus elastic fibre composite score of the papillary dermis and elastic fibre composite score of the reticular dermis; model 4: as model 3 plus wrinkle grade. Epidermal p16INK4a positivity: number of cells staining positive for p16INK4a per mm length of the epidermal-dermal junction, dermal p16INK4a positivity: number of cells staining positive for p16INK4a per 1 mm<sup>2</sup> dermis

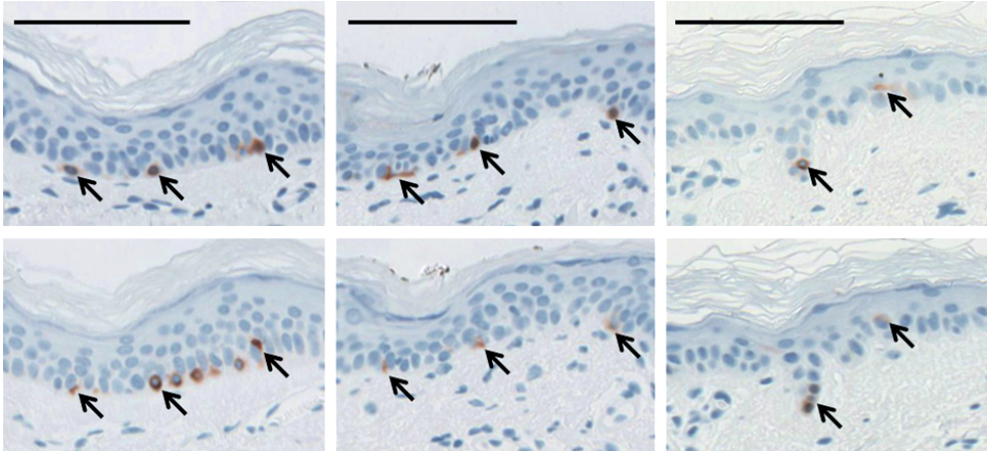


**Figure 3.** Staining for P16INK4a and MelA in adjacent skin sections from 3 participants. Skin sections from each participant (columns) were stained for p16INK4a (top images) and MelA (bottom images). The p16INK4a positive cells (arrows in top images) co-localised with MelA positive staining (arrows in bottom images); black line represents 100 $\mu$ m.

We next examined whether the p16INK4a positive epidermal cells were melanocytes. All p16INK4a positive cells (n=23 for three participants selected at random from those with high numbers of p16INK4a epidermal positivity) were located adjacent to the basement membrane and were S100 positive (data not shown). Epidermal p16INK4a positive cells were also observed to co-localise to MelA positive cells in adjacent 4  $\mu$ m skin biopsy sections (Figure 3).

## Discussion

Firstly, we demonstrated an association between epidermal and dermal p16INK4a positivity in the upper-inner arm with local elastic fibre morphology in both layers of the dermis. Secondly, and independently of the associations described above, we found significant associations between p16INK4a positivity in the epidermis, but not dermis, with a higher wrinkle grading and higher perceived age.

With age, greater numbers of senescent cells are observed in mice and human tissues<sup>2,6,7,33</sup>, due to an increase in senescent cells per se and/or failure to eliminate such cells by apoptosis or through clearance by the immune system. We found that epidermal p16INK4a positivity in the skin was associated with elastic fibre morphology analogous to changes with chronological age<sup>15</sup>. Of note, some of the associations were significant only after adjustment for potential confounders, highlighting the importance of external factors such as sun exposure and smoking. This association was particularly strong between elastic fibre characteristics in the

papillary dermis nearest the p16INK4a positive epidermal cells and less strong in the reticular dermis, and vice versa for dermal p16INK4a positivity. This suggests an interaction between the localization of p16INK4a positive cells and elastic fibre structure. We speculate that this link could be explained by the effects of the senescence associated secretory phenotype (SASP)<sup>34,35</sup>, since the factors secreted by senescent cells are likely to affect the surrounding tissue more than tissue located further away. In support of this, clearance of p16INK4a positive cells in progeroid mice delayed the onset of age-related diseases<sup>14</sup> and silencing p16INK4a in living skin equivalent models transformed the morphology of aged skin towards a younger phenotype<sup>36</sup>, although the p16INK4a positive cells in the skin equivalent were keratinocytes rather than melanocytes. Due to the cross-sectional nature of the study however, we cannot rule out that the number of p16INK4a positive cells are purely reflecting the degree of ageing rather than a direct influence of the SASP on the dermis.

Perceived age has been previously linked to ageing: it predicts survival<sup>24</sup> and links to pathology such as carotid atherosclerosis. Here, epidermal p16INK4a positivity associated with wrinkle grading and perceived age, independently of the associations between elastic fibre morphology and p16INK4a positivity. Although the association between epidermal p16INK4a positivity and perceived age is attenuated after adjusting for the wrinkling grading (because of the correlation between wrinkling and perceived age), a trend still exists indicating that epidermal p16INK4a is also associated with non-wrinkling facial aging features. In the dermis, a trend between p16INK4a positivity and perceived age was found after adjustment for the wrinkle grading, indicating that fibroblast p16INK4a positivity in a sun-protected site reflects the non-wrinkle components of perceived age such as face shape changes with age<sup>16,19</sup>. The reason for the differing associations with perceived age of epidermal and dermal p16INK4a positivity is unclear. However, in sun-exposed sites large dermal changes are associated with skin wrinkling; hence, it could be that the number of p16INK4a positive fibroblasts in sun-exposed skin is more strongly associated with facial wrinkling, but this now needs testing.

Previously we have suggested that the p16INK4a positive epidermal cells were likely melanocytes<sup>8</sup>. In agreement with previous observations<sup>32</sup> all p16INK4a positive cells in the epidermis were S100 positive, coincided with MelA staining in adjacent skin sections, and were located predominately along the basal membrane indicating that the cells were primarily melanocytes. This supports the importance of p16INK4a in melanocyte senescence, as senescence is an important tumour suppression mechanism<sup>37</sup>, p16INK4a expression loss associates with melanoma progression<sup>38</sup> and DNA mutations in the p16INK4a locus have been found in familial melanoma cases<sup>39</sup>. Here, the numbers of p16INK4a positive melanocytes were a good indicator of the extent of facial ageing. This result may reflect the

efficiency of cellular mechanisms (e.g. DNA repair) required for protection of melanocytes to pro-ageing factors across the body. However, the link between p16INK4a expressing cells in sun-protected skin with facial ageing could also be due to variations within the LLS cohort of environmental exposures such as diet <sup>40</sup> and physical activity <sup>33;41</sup>. Thus, further work is required to determine what mechanisms are driving the link between p16INK4a positive melanocytes in human arm skin and facial ageing.

One of the limitations of our study is the cross-sectional design of the study, which does not allow for conclusions on causal rather than associative relationships. In addition, the subjects were members of long-lived families which we have previously shown to have lower numbers of p16INK4a positive cells in skin <sup>8</sup>. However, all results were adjusted for long-lived family member status. Another potential issue is that the biopsies were taken from the upper-inner arm, while perceived age and the wrinkle grading were derived from the face. However, we believe it a striking observation that despite this lack of direct spatial relationship, p16INK4a positivity within arm skin is significantly linked to a more global phenomenon such as perceived age. The observation that p16INK4a positive cells are primarily melanocytes within the skin samples in our study is supported by the fact the p16INK4a staining was seen exclusively in S100 positive cells. Also, melaA staining of these p16INK4a positive cells in consecutive sections was observed. However, larger numbers of subjects would be required to conclusively rule out the presence of p16INK4a positive keratinocytes in sun-protected skin. Finally, due to the large number of participants we only used one, albeit widely used and validated <sup>1;2;7;33</sup>, marker for cellular senescence which means we cannot definitively assign these results to cell senescence. Including other markers, such as SA $\beta$ -gal or DNA damage foci, would have provided more evidence to term the p16INK4a positive cells senescent. However, irrespective of whether cells expressing p16INK4a *in situ* are truly senescent or not, p16INK4a positive cells in human skin are indicative of local elastic fibre morphology and facial ageing, and thus be considered a marker of global skin ageing.

This is the largest study of cellular senescence in skin to-date (n=178 participants) and participants of the LLS were extensively phenotyped which allowed us to adjust the findings for potential confounders. Within these participants we previously reported that p16INK4a positivity in the skin was lower in long-lived family member than in their partners <sup>8</sup>. Now, to the best of our knowledge we are the first to show a significant link between p16INK4a positivity in one body site with signs of visible ageing (wrinkle grading and perceived age) in another, independently of long-lived family member status and of chronological age. P16INK4a positive cells in the skin were also linked to local elastic fibre morphology in a manner resembling the effects of chronological age. In addition, we show that the numbers of p16INK4a positive cells in the epidermis of sun-protected skin are restricted to the

melanocyte cell population, highlighting the importance of the p16INK4a cell cycle checkpoint in melanocyte ageing. This study shows that p16INK4a positivity is, apart from a cellular senescence phenomenon and being linked to familial longevity, also strongly linked to human skin and facial ageing *in vivo*. Further work should focus on the causal factors driving the link between p16INK4a positive cells and skin ageing. Additionally, the importance of cellular senescence in human ageing should be explored in other tissues, to study whether it is a ubiquitous phenomenon of *in vivo* human ageing.

## **Acknowledgements**

We would like to thank Nicole Hudson, Sharon Catt and Michael van Ginkel for the elastic fibre measures, Barbara Strongitharm and William Parish for the p16INK4a counts, Claire Brock for the MelA and p16INK4 co-staining, Peter Murray and Cyrena Tomlin for help creating the perceived ages, Tamara Griffiths and Stephanie Ogden for the wrinkle grading, Corine de Koning-Treurniet and Ton de Craen for the acquisition of photographs, and Joke Blom and Corine de Koning-Treurniet for their help in skin biopsy processing.

This study was supported by the Innovation Oriented research Program on Genomics (SenterNovem; IGE01014, IGE5007), the Centre for Medical Systems Biology (CMSB), the Netherlands Genomics Initiative/Netherlands Organization for scientific research (NGI/NWO 05040202, 050-060-810 (NCHA)), Unilever, the EU funded Network of Excellence Lifespan (FP6 036894) and the National Institute on Aging (NIA P01 AG031862). Individual co-authors were funded by: the Netherlands Genomics Initiative (NCHA 050-060-810) [PES] and T32HL007751 - NIH Training Grant in Mechanisms of Vascular Disease [JSP].

**Supplementary table 1.** Skin morphology dependent on tertiles of epidermal P16INK4a positivity.

	Tertiles of epidermal p16INK4a positivity			P for trend
	Low ≤0.30 (N=59)	Middle 0.30-1.30 (N=60)	High ≥1.30 (N=59)	
<b>Epidermis</b>				
Thickness, $\mu\text{m}$				
Model 1	39.0 (0.87)	39.8 (0.85)	41.2 (0.87)	0.084
Model 2	39.5 (1.06)	39.9 (1.15)	41.6 (1.14)	0.108
Curvature				
Model 1	827 (8.56)	844 (8.36)	843 (8.58)	0.182
Model 2	817 (11.1)	831 (12.0)	839 (11.9)	0.097
<b>Papillary dermis (layer 1)</b>				
Area covered by fibres, $\mu\text{m}^2$ <sup>a</sup>				
Model 1	23.3 (2.89)	24.5 (2.82)	37.2 (2.90)	0.001
Model 2	21.4 (3.54)	23.0 (3.85)	39.6 (3.80)	<0.001
Number of elastic fibres				
Model 1	43.1 (5.41)	45.1 (5.28)	68.8 (5.42)	0.001
Model 2	41.0 (6.41)	43.8 (6.96)	75.6 (6.89)	<0.001
Area covered by a single fibre, $\mu\text{m}^2$				
Model 1	27.3 (1.10)	27.7 (1.07)	32.6 (1.10)	0.001
Model 2	26.3 (1.32)	27.3 (1.43)	33.2 (1.42)	<0.001
Length of a fibre, $\mu\text{m}$				
Model 1	15.0 (0.47)	15.8 (0.46)	17.3 (0.47)	0.001
Model 2	14.7 (0.57)	15.7 (0.61)	17.7 (0.61)	<0.001
Thickness of a fibre, nm				
Model 1	1920 (28.1)	1866 (27.4)	1955 (28.1)	0.413
Model 2	1912 (37.6)	1849 (40.8)	1957 (40.4)	0.355
Curl of a fibrea				
Model 1	925 (6.26)	914 (6.11)	904 (6.27)	0.021
Model 2	922 (7.79)	910 (8.45)	894 (8.36)	0.004
<b>Reticular dermis (layers 2-5)</b>				
Area covered by fibres, $\mu\text{m}^2$ <sup>a</sup>				
Model 1	62.7 (3.65)	64.1 (3.62)	75.1 (3.66)	0.020
Model 2	61.0 (4.58)	62.4 (5.00)	76.4 (4.92)	0.008
Number of elastic fibres				
Model 1	95.7 (4.29)	103 (4.25)	112 (4.30)	0.010
Model 2	92.3 (5.30)	99.6 (5.79)	112 (5.70)	0.003
Area covered by a single fibre, $\mu\text{m}^2$				
Model 1	48.4 (1.85)	47.1 (1.83)	51.5 (1.85)	0.245
Model 2	47.6 (2.23)	47.3 (2.44)	52.5 (2.40)	0.080

**Supplementary table 1.** (continued)

	Tertiles of epidermal p16INK4a positivity			P for trend
	Low ≤0.30 (N=59)	Middle 0.30-1.30 (N=60)	High ≥1.30 (N=59)	
Length of a fibre, $\mu\text{m}$				
Model 1	20.7 (0.56)	20.7 (0.56)	21.8 (0.57)	0.148
Model 2	20.1 (0.69)	20.5 (0.75)	21.9 (0.74)	0.035
Thickness of a fibre, nm				
Model 1	2173 (20.6)	2159 (20.4)	2192 (20.6)	0.518
Model 2	2186 (26.6)	2184 (29.0)	2220 (28.6)	0.306
Curl of a fibre				
Model 1	907 (5.47)	914 (5.43)	907 (5.49)	0.993
Model 2	909 (7.41)	918 (8.09)	908.9 (7.97)	0.980

All values are given as estimated mean (standard error).  $a = \times 10^3$ . Linear mixed model: model 1: adjustment for age, sex and long-lived family member status; model 2: as model 1 plus skin tanning type, sunbed use, sun exposure, smoking, number of cardiovascular and metabolic diseases and body-mass index. Independent variable: tertiles of p16INK4a positivity, dependent variables: skin morphology characteristics. Tertiles of p16INK4a positive epidermal cells: lowest  $\leq 0.30$  (median = 0.00), middle 0.30–1.30 (median = 0.55), highest  $\geq 1.30$  (median = 3.09) cells per mm length of the epidermal–dermal junction.

**Supplementary table 2.** Skin morphology dependent on tertiles of dermal P16INK4a positivity.

	Tertiles of dermal p16INK4a positivity			P for trend
	Low ≤0.72 (N=59)	Middle 0.72-2.05 (N=60)	High ≥2.05 (N=59)	
<b>Epidermis</b>				
Thickness, $\mu\text{m}$				
Model 1	40.3 (0.87)	40.5 (0.86)	39.2 (0.86)	0.383
Model 2	41.1 (1.11)	40.3 (1.10)	39.2 (1.16)	0.139
Curvature <sup>a</sup>				
Model 1	835 (8.56)	845 (8.50)	835 (8.45)	0.968
Model 2	821 (11.6)	838 (11.5)	822 (12.1)	0.971
<b>Papillary dermis (layer 1)</b>				
Area covered by fibres, $\mu\text{m}^2$ <sup>a</sup>				
Model 1	23.6 (2.95)	32.7 (2.93)	28.6 (2.91)	0.251
Model 2	21.9 (3.91)	32.0 (3.86)	29.1 (4.08)	0.132
Number of elastic fibres				
Model 1	43.6 (5.51)	61.0 (5.47)	52.5 (5.44)	0.277
Model 2	41.9 (7.12)	60.7 (7.03)	55.9 (7.42)	0.108
Area covered by a single fibre, $\mu\text{m}^2$				
Model 1	26.8 (1.11)	30.7 (1.11)	30.2 (1.10)	0.036

**Supplementary table 2.** Skin morphology dependent on tertiles of dermal p16INK4a positivity. (continued)

	Tertiles of dermal p16INK4a positivity			P for trend
	Low ≤0.72 (N=59)	Middle 0.72-2.05 (N=60)	High ≥2.05 (N=59)	
Model 2	26.2 (1.45)	30.1 (1.43)	30.3 (1.51)	0.022
Length of a fibre, µm				
Model 1	14.9 (0.47)	16.4 (0.47)	16.7 (0.47)	0.007
Model 2	14.8 (0.61)	16.3 (0.61)	16.9 (0.64)	0.005
Thickness of a fibre, nm				
Model 1	1928 (28.2)	1931 (28.0)	1882 (27.8)	0.245
Model 2	1913 (40.0)	1924 (39.5)	1882 (41.7)	0.502
Curl of a fibrea				
Model 1	920 (6.29)	916 (6.25)	908 (6.21)	0.207
Model 2	915 (8.33)	910 (8.23)	902 (8.69)	0.180
<b>Reticular dermis (layers 2-5)</b>				
Area covered by fibres, µm <sup>2</sup> <sup>a</sup>				
Model 1	59.4 (3.65)	73.0 (3.60)	69.5 (3.61)	0.062
Model 2	56.5 (4.79)	72.5 (4.72)	70.6 (5.01)	0.017
Number of elastic fibres				
Model 1	92.9 (4.23)	114 (4.17)	104 (4.19)	0.083
Model 2	87.6 (5.50)	110 (5.42)	105 (5.75)	0.011
Area covered by a single fibre, µm <sup>2</sup>				
Model 1	44.9 (1.83)	51.3 (1.80)	50.8 (1.81)	0.025
Model 2	44.7 (2.31)	51.7 (2.28)	51.1 (2.42)	0.024
Length of a fibre, µm				
Model 1	19.9 (0.56)	21.5 (0.55)	21.8 (0.55)	0.013
Model 2	19.6 (0.71)	21.3 (0.70)	21.6 (0.75)	0.021
Thickness of a fibre, nm				
Model 1	2141 (20.4)	2205 (20.1)	2178 (20.2)	0.224
Model 2	2159 (27.6)	2225 (27.2)	2205 (28.8)	0.181
Curl of a fibrea				
Model 1	908 (5.49)	913 (5.41)	907 (5.43)	0.882
Model 2	912 (7.80)	914 (7.68)	908 (8.16)	0.678

All values are given as estimated mean (standard error). a=  $\times 10^3$ . Linear mixed model: model 1: adjustment for age, sex and long-lived family member status; model 2: as model 1 plus skin tanning type, sun bed use, sun exposure, smoking, number of cardiovascular and metabolic diseases and body-mass index. Independent variable: tertiles of p16INK4a positivity, dependent variables: skin morphology characteristics. Tertiles of p16INK4a positive dermal fibroblasts: lowest ≤0.72 (median=0.00), middle 0.72-2.05 (median=1.29), highest ≥2.05 (median 3.20) cells per 1mm<sup>2</sup> dermis.

## References

- (1) Rodier F, Campisi J. Four faces of cellular senescence. *J Cell Biol* 2011;192:547-556.
- (2) Krishnamurthy J, Torrice C, Ramsey MR et al. Ink4a/Arf expression is a biomarker of aging. *J Clin Invest* 2004;114:1299-1307.
- (3) Herbig U, Ferreira M, Condel L, Carey D, Sedivy JM. Cellular senescence in aging primates. *Science* 2006;311:1257.
- (4) Jayapalan JC, Ferreira M, Sedivy JM, Herbig U. Accumulation of senescent cells in mitotic tissue of aging primates. *Mech Ageing Dev* 2007;128:36-44.
- (5) Dimri GP, Lee X, Basile G et al. A biomarker that identifies senescent human cells in culture and in aging skin in vivo. *Proc Natl Acad Sci U S A* 1995;92:9363-9367.
- (6) Melk A, Schmidt BM, Takeuchi O, Sawitzki B, Rayner DC, Halloran PF. Expression of p16INK4a and other cell cycle regulator and senescence associated genes in aging human kidney. *Kidney Int* 2004;65:510-520.
- (7) Ressler S, Bartkova J, Niederegger H et al. p16INK4A is a robust in vivo biomarker of cellular aging in human skin. *Aging Cell* 2006;5:379-389.
- (8) Waaijer ME, Parish WE, Strongitharm BH et al. The number of p16INK4a positive cells in human skin reflects biological age. *Aging Cell* 2012;11:722-725.
- (9) Koppelstaetter C, Schratzberger G, Perco P et al. Markers of cellular senescence in zero hour biopsies predict outcome in renal transplantation. *Aging Cell* 2008;7:491-497.
- (10) Westhoff JH, Hilgers KF, Steinbach MP et al. Hypertension induces somatic cellular senescence in rats and humans by induction of cell cycle inhibitor p16INK4a. *Hypertension* 2008;52:123-129.
- (11) Verzola D, Gandolfo MT, Gaetani G et al. Accelerated senescence in the kidneys of patients with type 2 diabetic nephropathy. *Am J Physiol Renal Physiol* 2008;295:F1563-F1573.
- (12) Minamino T, Miyauchi H, Yoshida T, Ishida Y, Yoshida H, Komuro I. Endothelial cell senescence in human atherosclerosis: role of telomere in endothelial dysfunction. *Circulation* 2002;105:1541-1544.
- (13) Tsuji T, Aoshiba K, Nagai A. Alveolar cell senescence in patients with pulmonary emphysema. *Am J Respir Crit Care Med* 2006;174:886-893.
- (14) Baker DJ, Wijshake T, Tchkonja T et al. Clearance of p16Ink4a-positive senescent cells delays ageing-associated disorders. *Nature* 2011;479:232-236.
- (15) Waaijer ME, Gunn DA, Catt SD et al. Morphometric skin characteristics dependent on chronological and biological age: the Leiden Longevity Study. *Age (Dordr )* 2012;34:1543-1552.
- (16) Gunn DA, Rexbye H, Griffiths CE et al. Why some women look young for their age. *PLoS One* 2009;4:e8021.
- (17) Gosain AK, Klein MH, Sudhakar PV, Prost RW. A volumetric analysis of soft-tissue changes in the aging midface using high-resolution MRI: implications for facial rejuvenation. *Plast Reconstr Surg* 2005;115:1143-1152.
- (18) Ozdemir R, Kilinc H, Unlu RE, Uysal AC, Senoz O, Baran CN. Anatomicohistologic study of the retaining ligaments of the face and use in face lift: retaining ligament correction and SMAS plication. *Plast Reconstr Surg* 2002;110:1134-1147.
- (19) Nkengne A, Bertin C, Stamatas GN et al. Influence of facial skin attributes on the perceived age of Caucasian women. *J Eur Acad Dermatol Venereol* 2008;22:982-991.
- (20) Takema Y, Hattori M, Aizawa K. The relationship between quantitative changes in collagen and formation of wrinkles on hairless mouse skin after chronic UV irradiation. *J Dermatol Sci* 1996;12:56-63.
- (21) Griffiths CE. The clinical identification and quantification of photodamage. *Br J Dermatol* 1992;127 Suppl 41:37-42.
- (22) Warren R, Gartstein V, Kligman AM, Montagna W, Allendorf RA, Ridder GM. Age, sunlight, and facial skin: a histologic and quantitative study. *J Am Acad Dermatol* 1991;25:751-760.
- (23) Gordon JR, Brieve JC. Images in clinical medicine. Unilateral dermatoheliosis. *N Engl J Med* 2012;366:e25.
- (24) Christensen K, Thinggaard M, McGue M et al. Perceived age as clinically useful biomarker of ageing: cohort study. *BMJ* 2009;339:b5262.
- (25) Noordam R, Gunn DA, Tomlin CC et al. High serum glucose levels are associated with a higher perceived age. *Age (Dordr )* 2013;35:189-195.

- (26) Noordam R, Gunn DA, Tomlin CC et al. Cortisol serum levels in familial longevity and perceived age: the Leiden longevity study. *Psychoneuroendocrinology* 2012;37:1669-1675.
- (27) Gunn DA, de Craen AJ, Dick JL et al. Facial appearance reflects human familial longevity and cardiovascular disease risk in healthy individuals. *J Gerontol A Biol Sci Med Sci* 2013;68:145-152.
- (28) Kido M, Kohara K, Miyawaki S, Tabara Y, Igase M, Miki T. Perceived age of facial features is a significant diagnosis criterion for age-related carotid atherosclerosis in Japanese subjects: J-SHIP study. *Geriatr Gerontol Int* 2012;12:733-740.
- (29) Gunn DA, Murray PG, Tomlin CC, Rexbye H, Christensen K, Mayes AE. Perceived age as a biomarker of ageing: a clinical methodology. *Biogerontology* 2008;9:357-364.
- (30) Schoenmaker M, de Craen AJ, de Meijer PH et al. Evidence of genetic enrichment for exceptional survival using a family approach: the Leiden Longevity Study. *Eur J Hum Genet* 2006;14:79-84.
- (31) Klaes R, Friedrich T, Spitkovsky D et al. Overexpression of p16(INK4A) as a specific marker for dysplastic and neoplastic epithelial cells of the cervix uteri. *Int J Cancer* 2001;92:276-284.
- (32) Pawlikowski JS, McBryan T, van TJ et al. Wnt signaling potentiates neovogenesis. *Proc Natl Acad Sci U S A* 2013;110:16009-16014.
- (33) Liu Y, Sanoff HK, Cho H et al. Expression of p16(INK4a) in peripheral blood T-cells is a biomarker of human aging. *Aging Cell* 2009;8:439-448.
- (34) Coppe JP, Patil CK, Rodier F et al. Senescence-associated secretory phenotypes reveal cell-nonautonomous functions of oncogenic RAS and the p53 tumor suppressor. *PLoS Biol* 2008;6:2853-2868.
- (35) Kuilman T, Peeper DS. Senescence-messaging secretome: SMS-ing cellular stress. *Nat Rev Cancer* 2009;9:81-94.
- (36) Adamus J, Aho S, Meldrum H, Bosko C, Lee JM. p16INK4A influences the aging phenotype in the living skin equivalent. *J Invest Dermatol* 2014;134:1131-1133.
- (37) Campisi J. Senescent cells, tumor suppression, and organismal aging: good citizens, bad neighbors. *Cell* 2005;120:513-522.
- (38) Keller-Melchior R, Schmidt R, Piepkorn M. Expression of the tumor suppressor gene product p16INK4 in benign and malignant melanocytic lesions. *J Invest Dermatol* 1998;110:932-938.
- (39) Platz A, Hansson J, Mansson-Brahme E et al. Screening of germline mutations in the CDKN2A and CDKN2B genes in Swedish families with hereditary cutaneous melanoma. *J Natl Cancer Inst* 1997;89:697-702.
- (40) Shi Q, Hubbard GB, Kushwaha RS et al. Endothelial senescence after high-cholesterol, high-fat diet challenge in baboons. *Am J Physiol Heart Circ Physiol* 2007;292:H2913-H2920.
- (41) Melk A, Tegtbur U, Hilfiker-Kleiner D et al. Improvement of biological age by physical activity. *Int J Cardiol* 2014;176:1187-1189.

